Magnetization of a superconductor: Results from the critical-state model

Z. Kozioł,* J. J. M. Franse, P. F. de Châtel, and A. A. Menovsky
Van der Waals-Zeeman Laboratorium, Universiteit van Amsterdam, Valckenierstraat 65, 1018 XE Amsterdam, The Netherlands
(Received 20 June 1994)

The field suppression of the critical current density in superconductors, j_c, is modeled within the critical-state theory by the modified Kim-Anderson relation, $j_c(B,T)=\alpha(T)/(B+h)^n$, with α, h, and n being phenomenological parameters. This quasistatic approach of analyzing the flux evolution in a sample under varying external field allows us to explain a few ubiquitous, experimentally known results: the occurrence of a peak in the $M(H)$ hysteresis at low fields and the saturation of the remanent magnetization as a function of sample size for larger sample sizes. In the present work, the critical-state concept is extended to describe the flux-profile evolution under temperature changes. Within this approach, the temperature dependences of the zero-field-cooled magnetization and of the remanent magnetization are calculated and compared with measurements performed on single crystals of $Bi_2Sr_2CaCu_2O_8$, UPt_3, and URu_2Si_2. This approach has been applied for computing magnetocaloric effects in a superconductor exposed to a changing external field. Estimates on the value and temperature dependence of the field for flux jumps are given for heavy-fermion superconductors and they are compared with the known results for URu_2Si_2.

I. INTRODUCTION

The critical current density belongs to the fundamental quantities determining the magnetization of superconductors. In type-I superconductors, it usually denotes the upper limit of the current density which can be passed through a material without energy losses in which case it is comparable to the depairing current density. In type-II materials, this upper limit for the current is never reached in practice since interaction of the current with vortex lines causes energy dissipation. Current-voltage characteristics are strongly nonlinear then. Usually, a rather sharp onset of resistance, defined as dE/dj, is observed at a certain critical value of the current, j_c. In order to model the magnetization behavior of superconductors characterized by strongly nonlinear $E(j)$ relations, Bean's critical-state model is used.[1,2] In this model, it is assumed that the current density can have but three values: j_c, $-j_c$, and 0. The critical current density is related to the width of the magnetic hysteresis.

The critical current depends strongly on details of the flux pinning. Various forms of critical-state models have been proposed for specific superconducting systems, where different types of defects have different pinning effects. Anderson[3] and Kim, Hempstead, and Strnad[4] modified the Bean model, suggesting that j_c should decrease with increasing local magnetic field and should have the form $j_c=\alpha/(h+B)$, where α and h are macroscopic material parameters, with h of the order of the thermodynamic critical field. A power-law field dependence of j_c was proposed by Irie and Yamafuji,[5] $j_c=\alpha/B^n$, where again, α and n characterize the pinning strength. Fietz *et al.*[6] found that their experimental results on Nb-Zr wires were excellently fitted with an empirical formula: $j_c=j_c(T)\exp(-B/h)$. The same form of $j_c(T,B)$ dependence is used sometimes when results on high-T_c superconductors are analyzed.[7] Recently, Xu, Shi, and Fox[8] showed that a generalized relation, which is a modified Kim-Anderson equation can unify the previous forms of the critical-state models, with the critical current density, $j_c(B)$, related to the curl of the magnetic induction, defined as

$$j_c(\mathbf{r})=\frac{\alpha}{[B(\mathbf{r})+h]^n}=|-(c/4\pi)\nabla\times\mathbf{B}| \ . \tag{1}$$

The exponent n in Eq. (1) depends on the details of flux pinning. A range of different cases, corresponding to $1/4<n<4$ has been derived from the collective flux-pinning theory by Jensen.[9] Equation (1) successfully explains the low-field electrodynamic properties of granular superconductors (the generation of higher harmonics in the ac susceptibility[10] and the dependence of the ac susceptibility on sample size[11]). It was used to model the dependence of the transport critical-current density on magnetic field and on the size of sintered $YBa_2Cu_3O_7$ and $Bi_2Sr_2CaCu_2O_8$ samples,[12] it fits well the magnetization of thin films of $YBa_2Cu_3O_7$,[13] with $n=0.3$. It models the low-field magnetization relaxation quite well, as shown by Xu *et al.*[14]

In high-T_c materials, due to a strong suppression of the critical current density by magnetic field, an apparent j_c value reaches zero at the irreversibility field $H_{\rm irrev}(T)$. An approximate scaling has been reported,[15,16] $j_c=j_c[H/H_{\rm irrev}(T)]$, in analogy to the behavior of conventional superconductors,[17] where j_c is found to depend on the ratio of the magnetic field and the second critical field, H/H_{c2}. A scaling of the magnetization hysteresis curve by the temperature-dependent field H_p, corresponding to the position of the maximum in $|M(H)|$, $M(H,T)=M[H/H_p(T)]/H_p(T)$, was observed as well.[18] These results confirm that the critical current density can be approximated by a function which is a product of

temperature- and field-dependent functions. Usually, a phenomenological result can be used for the temperature dependence of the critical current density, $j_c(T,H=0)=j_0(1-t^2)^m$, where t is the reduced temperature, $t=T/T_c$, and where the value for the exponent m as deduced from experiments is usually between 1 and 3.[13,19–21] For the depairing critical current density, this power should be 3/2.[21] For the pinning at low fields caused by spatial variation in the charge carrier mean free path, a power $m=2.75$ results from theoretical arguments and indeed this value has been observed recently by Griessen *et al.*[13] on $YBa_2Cu_3O_7$ thin films. When spatial variations of T_c are present, $m=1$ is expected near T_c.[13]

While there are many successful efforts of modeling the as susceptibility of superconductors within the critical-state concept, the behavior of the dc magnetization still awaits exploration. The publications on this subject by Krusin-Elbaum *et al.*,[19] by Matsushita *et al.*[22] and, recently, by Clem and Hao,[23] explain in particular many of the low-field properties, where effects of the finite value of H_{c1} and of the equilibrium magnetization of the Abrikosov lattice are crucial for understanding the temperature dependence of the field-cooled (FC) magnetization. Especially important is the prediction of an approximately field-independent magnetization in the field-cooled state, $M_{FC}(T)$, and of its suppression with the size of the sample. These results are found to be in a good qualitative agreement with experimental observations and reproduce well the functional dependences of M_{FC} on field and sample size. Still, discrepancies appear if an attempt is made for a quantitative analysis.[19] One of the reasons for these discrepancies is a neglect of the field suppression of the critical current density, while the magnetic induction, usually, changes strongly within the sample volume. Still, it is possible to apply these results in an approximate analysis of the experimental data, as recently shown by Huyn[24] with respect to the magnetization curves of $Bi_2Sr_2CaCu_2O_8$ and Nb_3Sn single crystals. A more exact description is achieved, however, when the field dependence of j_c is taken into account, as shown for instance by Xu.[25]

In this paper, the magnetic properties of the heavy-fermion materials UPt_3 and URu_2Si_2 and of the high-T_c superconductor $Bi_2Sr_2CaCu_2O_8$ are analyzed. The main differences between these superconductors are the specific, material-dependent parameters that describe the field and temperature dependences of the critical current density as well as the absence of an irreversibility field in the case of heavy-fermion compounds. In heavy-fermion superconductors, the reported field-cooled magnetization is so small that often it is not observed at all, as in the measurements presented in this paper. In the experimental cases which are considered here, the first critical field is many times lower than the field for the first full flux penetration into the sample. In $Bi_2Sr_2CaCu_2O_8$ it is of the order of 10^2 G, in URu_2Si_2 it is less than 30 G,[20] while in UPt_3, according to different estimates, it is of the order of 10 G. Hence, a possible correction of the model due to a finite value of H_{c1} is negligible when the measurements of the zero-field-cooled (M_{ZFC}) and remanent magnetization (M_{rem}), performed in fields a few times larger than H_{c1}, are discussed. Similarly, the experimental results presented here do not require us to take into account the finite value of the equilibrium magnetization. The attention is directed towards a discussion of the zero-field-cooled magnetization and the remanent magnetization. Extending the theory by considering the dependence of the critical current density on the magnetic induction allows us to reproduce well the field dependence of the zero-field-cooled magnetization, especially significant near T_c.

A model of the history-dependent effects is proposed which follows from experimental observations, as, e.g., analysis of the remanent magnetization, $M_{rem}(T)$. The external field (applied well above T_c) in which the sample is cooled down, is removed at low temperature and subsequently the measurements are carried out while slowly heating the sample. It is found that the remanence is determined in a unique way by the ratio of H and $H^*(T)$, where $H^*(T)$ is the field for the first full flux penetration into the sample center at the temperature T. The field H^* is related to the critical current density is comparable to the field, where the maximum in $|M(H)|$ is observed. The proposed interpretation leads to an extension of the critical-state concept to situations where a change of temperature has a similar effect on the flux-profile evolution as a change of magnetic field. This idea, in fact, is used in the original theory of Krusin-Elbaum *et al.*[19] However, it was not expressed explicitly by them. Here, it is explained how it follows from the experimental observations.

Another phenomenon modeled here is the magnetocaloric effect, recently studied successfully on high-T_c materials[26–30] and observed also in heavy-fermion superconductors[20] through the appearance of magnetic flux jumps. The calculated results on the temperature changes under a field sweep fits well the experimental observation.[30] The critical-state model, extended to the description of the flux-profile evolution induced by changes of temperature, allows us to further develop these results on the magnetocaloric effects, to such phenomena as flux jumps. Examples of the flux evolution during flux jumps are given. Estimates of the field for the first flux jumps, performed for heavy-fermion superconductors, are compared with published results. Possible further experiments are described which would resolve the question of the low-field anisotropy of magnetic response in unconventional superconductors.

II. EXPERIMENTAL DETAILS

The experimental results reported in this paper were obtained on single-crystalline samples. The $Bi_2Sr_2CaCu_2O_8$ sample is characterized by a sharp superconducting transition in the ac susceptibility. Its size is $4.8\times6.6\times1.75$ mm^3 and its T_c value is 87 K. The crystallographic c axis is perpendicular to the large surface of the sample and this was the direction of the applied magnetic field. The URu_2Si_2 sample has a cube shape with an

edge size of 3 mm; the magnetic field was oriented along the crystallographic c direction. Some properties of the UPt_3 sample (containing 11% of boron) with a size $2\times0.3\times2.8$ mm^3, ($a\times b\times c$) are described in previous publications.[31,32] From measurements on URu_2Si_2 as well as on different UPt_3 samples of different shape and for different field orientation with respect to the crystallographic axes, one has to conclude that anisotropic effects occur in the magnetization of these compounds, as described elsewhere.[32]

For magnetization studies, a commercial Hall probe (supplied by Lake Shore Cryotronics, Inc.[33]) was used as a sensor of the magnetic field at the surface of a magnetized sample. Its sensitivity is 8 $\mu\Omega$/G. With the Linear Research resistance bridge LR-400, an excellent stability, linearity of response on field, and an extremely small temperature dependence of the background signal is obtained, which is essential in these kinds of applications of a Hall probe. At certain conditions, a resolution in field measurements of 10 mG is reached at low fields, decreasing to about 0.1 G at fields of a few tesla. This technique, with examples of other magnetization measurements, has been described by us previously.[34] Here, only essential details shall be given.

For measurements at temperatures above 4 K, the sample was mounted directly on the surface of the ceramic case. At low temperatures (below 1 K), the small heat released in the Hall sensor (the ac current amplitude is 10 mA) prevents its cooling down in a ^{3}He absorption-pump system. To avoid heating of the studied sample, the Hall sensor is thermally isolated from the variable-temperature Cu plate at which the sample is mounted by a vacuum space (with a distance between the sample and the surface of the sensor of about 1 mm).

The sensitive area of the Hall probe is about 1 mm in diameter which is comparable to the sample size. The measured stray field is well related to the magnetization of the sample. The linear dependence between this field and the magnetization of the sample has been verified in low fields and at low temperatures by measuring the virgin magnetization curve in the Meissner state. In this case, the measured magnetization, $4\pi M_{\rm exp}=H_S-H$, where H_S is the field registered by the Hall probe and H is the externally applied field, should be found to reflect perfect diamagnetism, i.e., $4\pi M=-H$. For instance, for the $Bi_2Sr_2CaCu_2O_8$ sample studied here, it is observed that $4\pi M_{\rm exp}=-0.39\cdot H$, indicating that in the given geometry the sample does not screen the field perfectly. The result of this calibration, $4\pi M=4\pi M_{\rm exp}/0.39=(H_S-H)/0.39$, is used at all fields, although it is exact only for the low-field measurements. In particular at large fields, for which the current density is the same in the whole sample volume, the linear relation is recovered between H_S-H and $4\pi M$, albeit with a proportionality coefficient slightly different from that one at low fields.

The magnetic field used for low-field measurements is generated by a coil wound of a superconducting wire in a copper matrix on the vacuum can which is immersed in liquid helium. The magnetic field of 375 Oe/A is obtained, which is sufficiently uniform in the center of the coil.

III. REMANENT MAGNETIZATION AND HISTORY-DEPENDENT EFFECTS

Discussing the experimental results reported in this paper, we use the calculations within the modified Kim-Anderson critical-state model. To simplify the problem, we assume that a sample of a plate-shape is used, of thickness $2D$, with the magnetic field applied parallel to its surface. We refer to the Appendix for explanations and the details.

Let us cool down a sample in the FC procedure in the field H from $T>T_c$ to $T<T_c$. The magnetization is small in the FC state, in particular in the case of UPt_3 and URu_2Si_2, and one can assume that the magnetic induction inside the sample is uniform and equal to the applied external field H. Reduction of the magnetic field to zero at $T<T_c$ results in the induction of a surface critical current. The shape of the resulting flux profile depends on the value of the field H. If this field in the FC procedure was smaller than H^*, as for curve (a) in Fig. 1, the induction B in the sample region close to its center remains unchanged and it starts to decrease at a certain position, $x>0$, reaching $B=0$ at the sample surface. If H was equal to H^*, as for curve (c) in Fig. 1, or higher than H^*, as for curve (d) in this figure, B changes from the value H^* at the center, to zero at the surface. It is interesting to note that the remanent magnetization is independent of the value of the magnetic field H, if this

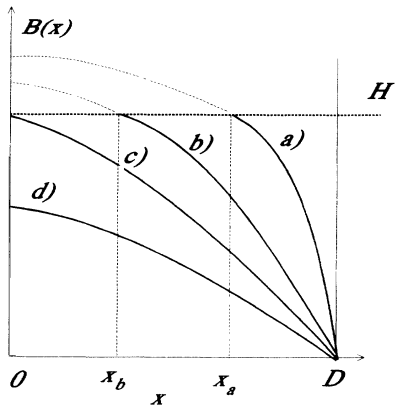

FIG. 1. Evolution of the field profile in the sample, represented by the solid lines, corresponding to measurements shown in Fig. 2. For $x<x_a$ and $x<x_b$ [curves (a) and (b), respectively] the magnetic induction is constant and equal to the initially applied field H. Curve (a) is obtained when the magnetic field $H<H^*(T_a)$ is removed at $T=T_a$, after FC. Curve (b) represents the changed field profile at $T_b>T_a$, after the temperature increased from T_a to T_b. If the temperature decreases from T_b to T_a then at T_a the flux profile will remain the same as the one represented by curve (b). Curves (c) and (d) are obtained when the field $H^*(T)$ becomes equal and subsequently higher than the field H removed at $T=T_a$, during temperature increase.

field is larger than H^*. The positive remanent magnetization is given then by

$$4\pi M_{\rm rem}=\frac{n+1}{n+2}\cdot\frac{(H^*+h)^{n+2}-h^{n+2}}{(H^*+h)^{n+1}-h^{n+1}}-h, \quad H>H^* . \tag{2}$$

The same equation is obtained for the remanent magnetization in the ZFC state, but for applied and removed external fields larger than about $2H^*$ ($2H^*$ holds for the Bean case while a little smaller maximal field is required if $n>0$). It is easy to check, using Eq. (2), that for $h \ll H^*$ the remanent magnetization $4\pi M_{\rm rem}$ is close to $(n+1)/(n+2)H^*$, while for $h \gg H^*$ it becomes similar as in the Bean model, i.e., $4\pi M_{\rm rem}\approx H^*/2$. If the magnetic field in the FC state is smaller than H^* at the temperature T where this field is removed, then the remanent magnetization is given by

$$4\pi M_{\rm rem}=\frac{n+1}{n+2}\cdot\frac{(H+h)^{n+2}-h^{n+2}}{(H^*+h)^{n+1}-h^{n+1}} -(H+h)\cdot\frac{(H+h)^{n+1}-h^{n+1}}{(H^*+h)^{n+1}-h^{n+1}}+H , \quad H<H^* . \tag{3}$$

In the present model, the field H^* weakly depends on D if n is large. As a result, the remanent magnetization is not scalable with the sample volume, as discussed also by Yeshurun *et al.*[35] and observed experimentally in $YBa_2Cu_3O_7$ (Ref. 36) and $Bi_2Sr_2CaCu_2O_8$ (Ref. 37) single crystals. It is possible to impose an even stronger, although less accurate, restriction on the upper limit of the remanent magnetization. The critical current density assumed here, defined by the modified Kim-Anderson relation, is overestimated for fields close to $H_{\rm irrev}$. If the existence of an irreversibility field is taken into account, the magnetic induction profile obtained after sweeping the field to some value $H>H_{\rm irrev}$ and subsequently to zero, has such a form that the maximal possible value for B inside a sample volume never exceeds $H_{\rm irrev}$. As a result, the remanent moment divided by the sample volume can never exceed $H_{\rm irrev}$, independent of the function $j_c(B)$ and the sample shape: $4\pi M_{\rm rem} \ll H_{\rm irrev}$ (in the Bean model this remanence is of the order of H^*, which is proportional to the linear size of the sample). This is the simplest argument for the existence of an upper limit of the remanent magnetization in high-T_c superconductors for any sample size. The function $M_{\rm rem}(D)$, initially linear for sufficiently small D, must become independent of D for sufficiently large D values.

The quite well-defined value of the maximal remanent magnetization, $H^*/2<4\pi M_{\rm rem}<(n+1)/(n+2)H^*$, gives the possibility of using the measurements of $M_{\rm rem}(T)$, as a method for sample characterization. This idea provided the inspiration for performing additional measurements of the remanent magnetization:

(i) as a function of applied and removed field, after cooling in zero-field;

(ii) as a function of field, with fields applied above T_c and removed at $T<T_c$.

It was found that the maximal remanent magnetization is the same in these cases, except for a small contribution from relaxation effects. The result of another kind of experiment is illustrated in Fig. 2, where the remanent magnetization is shown, measured after cooling the sample in field. At low temperature, the field is removed and the quasistatic remanent signal is measured during slowly heating the sample, with a temperature change rate of about 1 K/min. It should be stressed that the measured signal is very weakly dependent on the temperature sweep rate: changing the sweep rate a few times leads to results which are indistinguishable. The measured curves depend on the field H in which the sample has been cooled down; the remanent magnetization obtained after removing a field of 50 Oe is lower than the one remaining after 60 Oe (Fig. 2). However, they merge to one unique curve near T_c. Moreover, if the initially applied field is sufficiently large, the remanence becomes independent of the value of this field: the maximal possible remanence is reached then. This is indeed the same remanent signal as from measurements by methods (i) and (ii). At point A on curve (b) the temperature starts to decrease, reaching point B, and then the temperature increases again, up to point C, where a similar experiment is performed again. The results suggest that the shape of the flux profile after the decrease, and after the subsequent increase of temperature between points A-B and C-D, is unchanged. Similar history dependences were observed on URu_2Si_2 and UPt_3 samples in $M_{\rm rem}(T)$ and $M_{\rm ZFC}(T)$ measurements. This effect should be understood as a freezing of the flux profile after decreasing the temperature due to an increase of flux pinning. It is argued in the next sections that this concept should be used in the explanation of some of the flux-jump phenomena. The constant value of the magnetization after a decrease in temperature observed here is probably due to the large size of the sam-

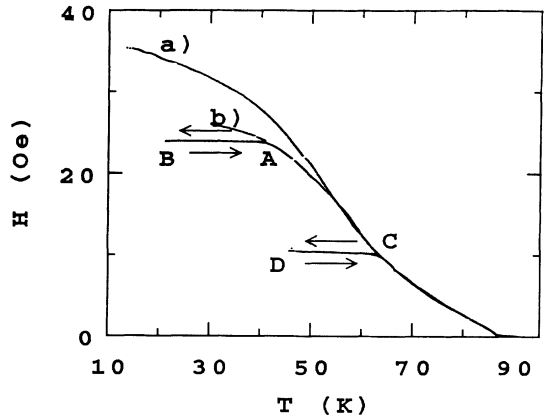

FIG. 2. The remanent magnetization of a $Bi_2Sr_2CaCu_2O_8$ single-crystalline sample measured by the Hall probe, after cooling the sample in field: (a) -60 Oe, (b) -50 Oe. At low temperature the field is removed, and the quasistatic remanent signal is measured during slowly heating the sample. At point A on curve (b) the temperature starts to decrease, reaching point B, and then the temperature increases again, up to the point C, where a similar experiment is performed again.

ples compared to the London penetration depth, since a similar investigation on powdered samples[38] gives different results. A similar conclusion follows from the work of Krusin-Elbaum *et al.*[19] and Clem and Hao.[23]

The experiments described by Fig. 2 call for the following mechanism of the flux-profile evolution under changes of field or temperature. Initially, when the field H ($<H^*$) is removed at the temperature T_a, as in Fig. 1, the flux distribution is represented by curve (a) in this figure. The supercurrent density, proportional to the gradient of the magnetic induction, has a critical value $j_c(B)$ for $x>x_a$, and is equal to zero for $x<x_a$. After an increase of the temperature, the pinning energy decreases, resulting in a decrease of the critical current density. A change of the supercurrent in the part of the sample volume with $x>x_a$ should cause a change of the magnetic induction in the region $x<x_a$, according to Ampères law. Such a change should, however, create an electric field, according to Faraday's rule and induce a finite current in the sample region $x<x_a$. Since the critical-state ansatz should work in this case, there is only a thin sample region at $x<x_a$, near to x_a, where the critical current density is generated, while at lower x values the supercurrent still remains equal to zero. As a result, at increasing temperature the self-consistently established critical-state region spreads out towards the sample center, as shown by curves (b) and (c) in Fig. 1. When the temperature reaches the value corresponding to curve (c) in this figure, the sample has the maximal possible remanent magnetization at this temperature. At further increasing the temperature, the field at the sample center will decrease according to the decrease of $H^*(T)$, as for curve (d) in Fig. 1.

The above explanation may be formulated by a mathematical formula:

$$H_0+\int_{x_0}^{D}\left[\frac{dB}{dx}\right]dx=H\ , \tag{4}$$

which expresses the condition of continuity of the magnetic field at the sample surface. In Eq. (4), H_0 is the field at the sample inside (in the considered case, it is equal to the initially applied field) and H is equal to the magnetic field at the sample surface (here it is equal to zero). The quantity dB/dx is just $(4\pi/c)j_c$, where j_c depends on temperature and magnetic field. Hence, we assume that both during change of external field and during increase of temperature the current density which flows in a superconductor has the maximal possible value, i.e., it is equal to the critical current density $j_c(T,B)$. The edge of the flux front, x_0, should be found from the condition that Eq. (4) is fulfilled.

Figure 3(a) shows the results of experiments performed on the URu_2Si_2 sample. The remanent magnetization obtained in different fields is represented by the circles which merge together near T_c, since the maximal remanent magnetization is reached then. By means of Eq. (2) that relates the maximal remanent magnetization to $j_c(T,B)$, an attempt was made to fit the experimental data. The following, phenomenological description for the temperature dependence of the critical current density was used: $j_c(T,H=0)=j_0(1-t^2)^m$, where $t=T/T_c$, $T_c=1.14$ K. It was found that with $m=1.5$ the results are well described with $j_0=18\,300$ A/cm^2, if a sample size with $D=0.1$ cm is assumed. The field dependence of $j_c(B)$ was assumed to be given by the Kim-Anderson formula, with $n=0.3$ and $h=90$ G. The calculated maximal remanent magnetization is given by the dotted line in Fig. 3(a). At low temperatures, it was not possible to measure the maximal remanent signal, since the maximal field available in the experimental setup (506 Oe) is not sufficient to induce the critical state in the whole sample volume. For our case, i.e., for $H<H^*(T)$, the magnetization is given by Eq. (3) and the calculated results are represented by the solid lines. The agreement between calculations and measurements is very good, despite the crude assumptions.

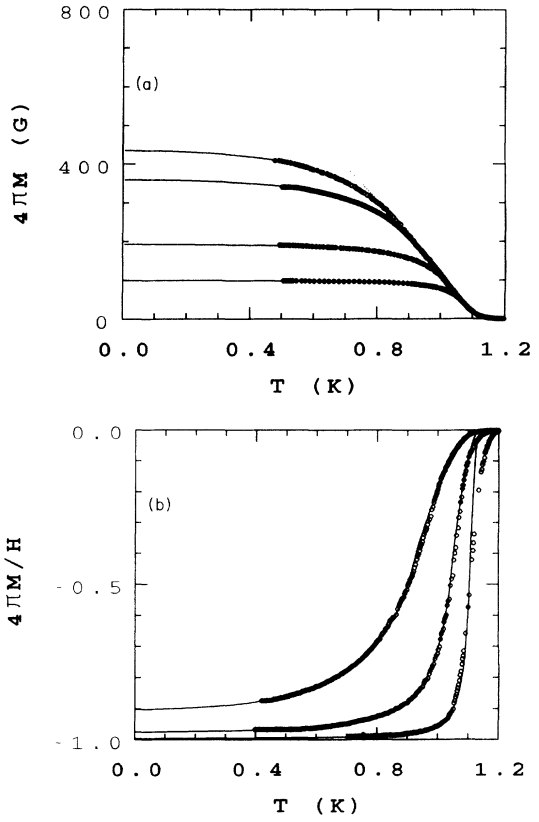

FIG. 3. Remanent magnetization (a) and ZFC magnetization (b) of a URu_2Si_2 single-crystalline sample. The solid lines and the dotted line represent calculations, while symbols are experimental results. The measurements were performed during slowly heating the sample after the field is removed at low temperature (at about 500 mK), for fields equal to 506, 400, 200, and 100 Oe, for the data from top to bottom, respectively. The solid lines are calculated for j_c given by $j_c(T,H=0)=18\,300$ A/cm^2 $(1-t^2)^{1.5}$, with $T_c=1.14$ K, $n=0.3$, and $h=90$ G. The dotted line represents the maximal possible remanent magnetization for this sample. For the ZFC mode the measurements were performed in fields of 300, 100, and 20 Oe, from top to bottom, respectively.

Similar calculations were performed for the ZFC magnetization. For applied fields H lower than H^*, the magnetization is given by Eq. (A4), and for $H > H^*(T)$ by Eq. (A5). A comparison with experiments is made in Fig. 3(b). Here, the quality of the fit is not so good, especially near T_c, which should be attributed mainly to a very approximate form of the assumed dependence of the supercurrent on the field. A similar analysis has been carried out for a UPt_3 sample. Figure 4(a) compares the remanent magnetization measured for three different fields. The largest field, $H = 182$ Oe, is higher than H^* at the lowest investigated temperature. Hence, $M_{rem}(T)$ data for that field represent the maximal possible remanence. The calculations, shown by the solid lines, were performed for $j_c(T, H=0) = j_0[1-(T/T_c)^2]^m$, with $j_0 = 3400$ A/cm^2 and $D = 0.1$ cm which is a very approximate estimate of the absolute value of the critical current density, since the sample orientation with respect to the field direction is not convenient for performing exact calculations. The Kim-Anderson parameters were the following: $n = 0.5$, $h = 10$ G. The value of 2 for the exponent m, used here, is larger than that in Ref. 20, where a similar form of the $j_c(T)$ dependence is considered. Here, an attempt was made to find a good description of the results for temperatures near T_c, while in Ref. 20 a fitting over a broader temperature range is shown. Moreover, it should be expected that the existence of a second phase transition in this unconventional superconductor, which occurs at $T^{minus} \approx T_c - 60$ mK could influence the $j_c(T)$ dependence. In that case the simple form of $j_c(T)$ is not suitable for fitting the results near T_c. While the agreement between measured and calculated curves for $M_{rem}(T)$ is rather good, the calculations for $M_{ZFC}(T)$, as shown in Fig. 4(b), are not reproducing so well the experimental curves, especially near T_c and at lower fields. However, the field suppression of the supercurrent is still following the calculations very well.

In Fig. 5, the scaling of the magnetization of the UPt_3 sample is presented. It is obtained in the following way. The solid line presents the virgin magnetization curve measured at $T = 448$ mK, while the circles have been determined from a large number of $M_{ZFC}(T)$ measurements performed in different fields. Then, for different temperatures (370 mK $< T <$ 480 mK, with steps of 2 mK) the $M_{ZFC}(H;T)$ data are collected and renormalized: the magnetization and field are multiplied by the same number (dependent on temperature), which gives the best coincidence with the magnetization curve at 448 mK. The good coincidence of all these data shows that the parameter n in the Kim-Anderson formula weakly depends on temperature in the investigated temperature range (the parameter h has a rather weak influence on the shape of magnetization curves) and supports the already explained hypothesis about the equivalence between the critical-state profiles in $M_{ZFC}(T)$ measurements and those established in $M(H)$ experiments. A similar scaling of the $M(H)$ curves measured on a Tl-based ceramic system has been reported recently by Wolfus *et al.*[18] and on $YBa_2Cu_3O_{7-x}$ single crystals by Oulssena *et al.*,[39] while for $Bi_2Sr_2CaCu_2O_8$ thin films the flux-pinning-force scaling was determined by Yamasaki *et al.*[16]

It has been established[40] that the following relation holds for measurements of $M_{rem}(T)$, $M_{ZFC}(T)$, and

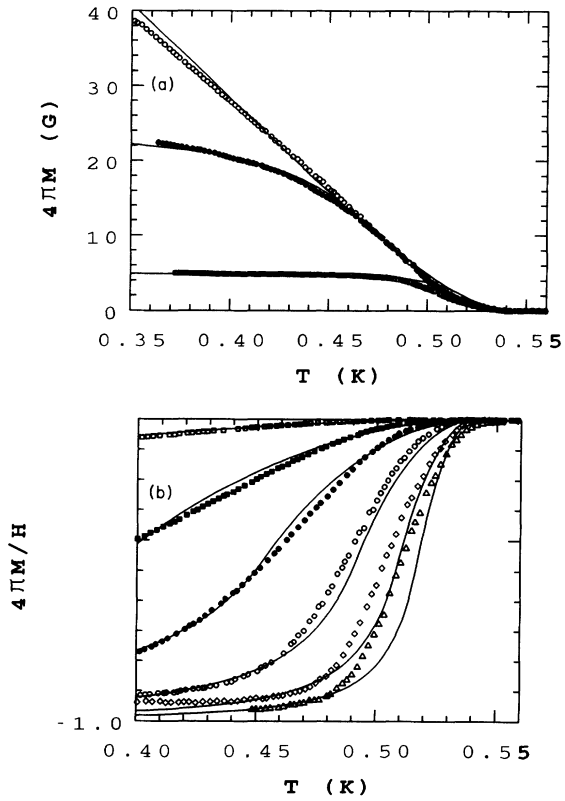

FIG. 4. (a) Remanent magnetization of a UPt_3 sample measured after removing the fields of 182, 25, and 5 Oe, from top to bottom, respectively. (b) Dc susceptibility, $M_{ZFC}(T)/H$, for fields 182, 50, 25.1, 10.5, 5, and 3 Oe, from top to bottom, respectively. The solid lines are calculated with $j_c = 3400$ A/cm^2 $[1-(T/T)^2]^2$, where $T_c = 546$ mK. The Kim-Anderson parameters assumed are $n = 0.5$, $h = 10$ G.

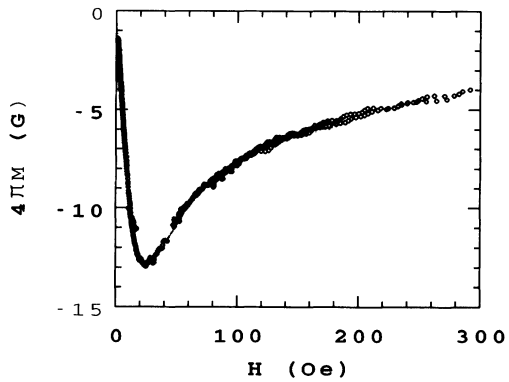

FIG. 5. Scaling of the $M_{ZFC}(T)$ curves for UPt_3, as given in Fig. 4(b), to the virgin magnetization curve (solid line) determined at $T = 448$ mK. The magnetization data M_{ZFC} and the field H, in which $M_{ZFC}(T)$ is measured, are multiplied by the same temperature-dependent number in order to reach coincidence with the $M(H)$ curve obtained at $T = 448$ mK.

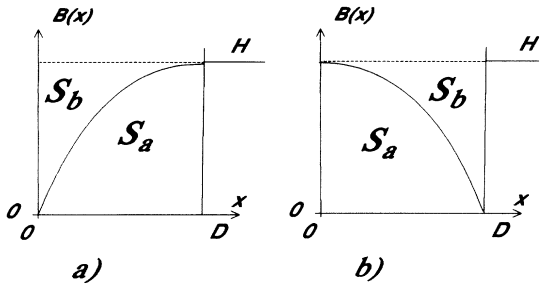

FIG. 6. (a) The flux profiles when the field $H=H^*$ is applied after cooling in zero field [or when temperature in ZFC measurements reaches the value T^*, defined by $H^*(T^*)=H$]. (b) The flux profile after cooling in field H, and removing this field at temperature T^*. In case (a) $M_{\rm ZFC}$ is proportional to the surface S_b, while in case (b) $M_{\rm rem}$ is proportional to the surface S_a.

$M_{\rm FC}(T)$: $M_{\rm rem}(T)=M_{\rm FC}(T)-M_{\rm ZFC}(T)$. This relation, however, originates from a phenomenological result for spin glasses[41] and has a limited range of validity, as noticed by Clem and Hao.[23] In the theory of Krusin-Elbaum *et al.*[19] and Clem and Hao[23] it is restricted to low fields and low temperatures. In the case of URu_2Si_2 and UPt_3 samples, the field-cooled magnetization is not observed at all. Hence, one should have $M_{\rm rem}(T)+M_{\rm ZFC}(T)=0$ in that case, since $M_{\rm FC}\approx 0$. A closer inspection of the data in Fig. 3 for URu_2Si_2, or in Fig. 4 for UPt_3, leads to the conclusion that at least near T_c this relation is not fulfilled. Within the critical-state model, the difference between the $M_{\rm rem}(T)$ and $|M_{\rm ZFC}(T)|$ values finds an explanation in a different flux distribution in ZFC and remanent-magnetization measurements, as shown schematically in Fig. 6. Using Eqs. (A4), (A5), (2), and (3), the sum $M_{\rm rem}(T)+M_{\rm ZFC}(T)$ has been calculated with the same parameters as used in the calculations presented in Fig. 3. The results are compared with the sum of the measured remanent magnetization and the ZFC magnetization (Fig. 7). A finite value

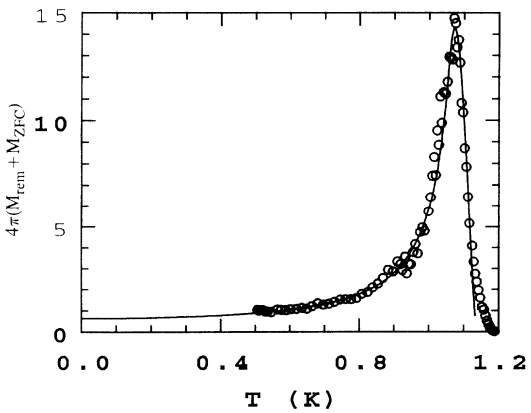

FIG. 7. The calculated (solid line) and experimental (circles) sum of $M_{\rm rem}(T)$ and $M_{\rm ZFC}(T)$. The measurements were performed at 100 Oe on a URu_2Si_2 sample. The same calculation parameters are used as those in Fig. 3.

of the signal is obtained at low temperatures, with a maximum near T_c, where $H^*(T)$ becomes comparable to H. A further inspection of Fig. 6 and analysis of Eqs. (A5) and (3) allows us to predict another relation: $4\pi M_{\rm rem}(T^*)-4\pi M_{\rm ZFC}(T^*)=H$, where the temperature T^* is given by the condition $H^*(T^*)=H$. It was checked that this relation holds for our experimental data, by comparing the H^* values determined by this method with the H^* values estimated from the $M(H)$ curves.

IV. THE FIELD-COOLED MAGNETIZATION

The observation of the field-cooled magnetization (known also as the field expulsion or Meissner effect) is treated as the evidence for the existence of superconductivity in any given material. Moreover, the value of the magnetization at low temperatures, relative to the one corresponding to total flux expulsion, is often taken as the fraction of the superconducting phase contained in the material. While this is the right view for compounds characterized by a low value of the Ginzburg-Landau parameter, one should note that the case of high-T_c and heavy-fermion superconductors is different.

In the literature, some conflicting results can be found for the value of the field-cooled magnetization of UPt_3, although it is always very small. On the basis of the theory of Krusin-Elbaum *et al.*[19] and Clem and Hao,[23] the low value of the field-cooled magnetization might be explained by a large value of the Ginzburg-Landau parameter in these materials and, consequently, by a low equilibrium magnetization of the Abrikosov lattice and a low value of the first critical field, as well as by a relatively strong flux pinning and large critical current densities. In the theory of Clem and Hao,[23] the field-cooled susceptibility, $4\pi M_{\rm FC}/H$, is approximately field independent and inversely proportional to the parameter $\gamma=(4\pi/c)j_cD/H_{c1}$, which for a sample of 1 mm size is equal to about 40 for UPt_3 and about 70 for URu_2Si_2. This could explain the absence of any signature of the field-cooled magnetization signal in our measurements on the heavy-fermion superconductors, since the resolution in this kind of measurements is limited to about 0.1 G. Further support for this explanation is found from the observation of Amato *et al.*[42] that the "Meissner fraction" from measurements on a bulk sample of UPd_2Al_3 amounts to 3% only, while a powderized sample gives 67% flux expulsion.

Recently, Braunisch *et al.*[43] reported the observation of the paramagnetic response (known also as Wohlleben effect) and unusual microwave absorption in certain granular samples of $Bi_2Sr_2CaCu_2O_8$, cooled in a very weak magnetic field. Due to the granularity of the system, it forms a network of Josephson junctions. It is supposed that besides the conventional junctions, it contains also, so-called, Π junctions.[44] This may occur for a *d*-wave order parameter. In that case, the current-phase relation has a sign that is different from that in a conventional superconductor. Ground states of the system are possible that break the time-reversal symmetry, i.e., states with a spontaneous supercurrent and a finite mag-

netization may occur. This fact is invoked[44] as an explanation of the Wohlleben effect observed by Braunisch *et al.* It is interesting to raise the question whether a possible formation of Π junctions in granular samples of UPt_3 could cancel the low-field Meissner effect, or whether the possible existence of *d*-wave pairing could be used for a description of the FC magnetization of single-crystalline samples.

The temperature dependence of $M_{FC}(T)$ is often used in attempts to determine that of the London penetration depth, λ_L. However, according to Clem and Hao,[23] the magnetization $M_{FC}(T)$ depends strongly on the critical current density, not only on the London penetration depth. For this reason, the existing results for λ_L for heavy-fermion superconductors, obtained from the field-cooled magnetization, have to be reanalyzed.

V. MAGNETOCALORIC EFFECTS UNDER A FIELD SWEEP

The relevance of studies of thermal effects in superconductors at varying magnetic fields is due to the technical importance of these phenomena in the perspective of possible applications. For high-T_c materials there are only preliminary, but interesting, experimental results on this subject.[26–30] Using the results obtained for the magnetic-field distribution in the modified Kim-Anderson critical-state model, in this section expressions are derived for the energy dissipated in a sample under changes of the magnetic field. Subsequently, the increase of temperature due to the released energy is computed. As a simple approximation of the experimental situation, it is assumed that changes of temperature do not influence the sample parameters: the specific heat of the sample and the critical current density are taken to be independent of temperature, except for the cases for which it is separately mentioned.

The power $dP(x)$ in a sample element of thickness dx, released during a field sweep dH/dt is given as the absolute value of the product of the electric field $E(x)$ induced by a change of the magnetic flux in a volume $(-x,x)$ and of the current density $j(x)$: $dP(x)=|E(x)j(x)|dx$, where $j(x)$ is obtained from Eq. (1), for the same geometry as discussed in previous sections whereas the electric field is given by

$$E(x)=-\frac{1}{c}\frac{d\Phi(x)}{dt}=-\frac{1}{c}\frac{d}{dt}\int_0^x B(x')dx' . \tag{5}$$

In the calculations, the attention is focused on the increasing, virgin branch of the magnetization curve $M(H)$. When the field H is lower than the field for first full penetration, H^*, one has by calculating the integral (5) for the field distribution given by Eq. (A1),

$$dP(x)=\frac{1}{4\pi}\cdot\frac{dH}{dt}\cdot\left[\frac{H+h}{B+h}\right]^n\cdot B(x)\cdot dx,\quad x>x_0(H) , \tag{6}$$

for the sample region where $B(x)\neq 0$, i.e., for $x>x_0(H)$. The edge of the flux profile in (6), x_0, is given by

$$\frac{x_0}{D}=\frac{(H^*+h)^{n+1}-(H+h)^{n+1}}{(H^*+h)^{n+1}-h^{n+1}} . \tag{7}$$

For $H>H^*$ one obtains

$$dP(x)=\frac{1}{4\pi}\frac{dH}{dt}\cdot\left[\frac{H+h}{B+h}\right]^n(B+h-\beta^{1/(n+1)})\cdot dx , \tag{8}$$

where β is given by Eq. (A2). It is easy to find from Eq. (8) that for $H\gg H^*$ the total power released in the sample volume is approximately proportional to the magnetization.

Integration of Eqs. (6) and (8) over the sample volume gives for the total power normalized by the sample volume, $P/2D$

$$P/2D=\frac{1}{4\pi}\frac{dH}{dt}\frac{(n+1)}{2\cdot[(H^*+h)^{n+1}-h^{n+1}]}(H+h)^nH^2,\quad \text{for } H<H^* \tag{9}$$

$$P/2D=\frac{1}{4\pi}\frac{dH}{dt}\frac{(n+1)}{2[(H^*+h)^{n+1}-h^{n+1}]}(H+h)^n \times\{(H+h)-[(H+h)^{n+1}-(H^*+h)^{n+1}+h^{n+1}]^{1/(n+1)}\}^2,\quad \text{for } H>H^* . \tag{10}$$

Figure 8 illustrates some cases of $4\pi P(H)/2D$ for different parameters n and h of the Anderson-Kim formula. Let us note that a sharp peak in $P(H)$ occurs at $H=H^*$, while in the magnetization curves the maximum is observed at the field H_p, which is lower than H^* (see, e.g., Fig. 16).

For calculating the sample temperature during a field sweep, it is assumed that the sample with a heat capacity C, where $C=2DC_v$ and C_v is the heat capacity per unit volume, is connected by a thermal contact of conductance κ with a bath of constant temperature. It is also assumed that the energy released during the field change increases the sample temperature with ΔT in a uniform way, i.e., that this energy is distributed equally over the whole sample volume. This is equivalent to the assumption of a good thermal conductivity of the sample, an assumption which is valid only for a limited number of experimental situations. In these circumstances one can write

$$C\cdot\Delta T(t)=\int_0^t P(t_1)dt_1-\int_0^t\Delta T(t_1)\kappa dt_1 , \tag{11}$$

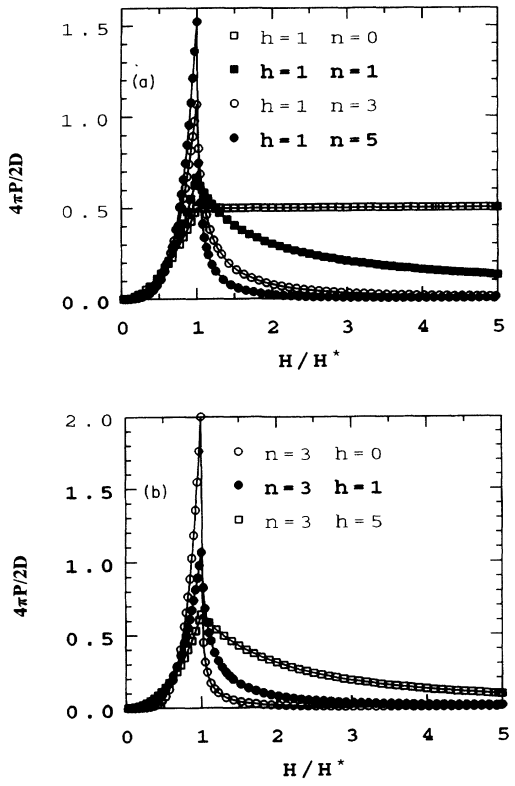

FIG. 8. The normalized power released during uniform (constant dH/dt) field increase for (a) $h=1$ and n ranging from 0 to 5, (b) $n=3$, but h changes from 0 to 5.

which may be written in the differential form

$$\frac{1}{C}P(t)=\frac{d\Delta T(t)}{dt}+\frac{\Delta T(t)}{\tau}\ , \tag{12}$$

with $\tau=C/\kappa$ being the relaxation time determining the heat exchange rate between the sample and the surrounding.

When τ is much larger than the experimental time scale (a time required to change the magnetic field for $\Delta H=H^*$) then the second term in (12) can be neglected and the temperature change weakly depends on the sample size: C and P are both proportional to D. A small dependence on D will persist only due to the dependence of H^* on the sample size.

Equation (12) can be used to determine $P(t)$ from the experimental $\Delta T(t)$ curve, provided the relaxation time τ and the heat capacity C of the sample are known. When the relaxation time is very large (much larger than the time of an experiment) then, obviously, a simpler approximation is valid: $P(t)/C=d\Delta T/dt$. In that case, the temperature change ΔT is independent of the way in which the field H has been applied, since neglecting the second term in Eq. (12) allows us to replace the integration of $P(t)$ over time by integration over field.

Let us solve Eq. (11) on $\Delta T(t)$ for an arbitrary function $P(t)$. One can find that the iteration method works: as a first step $\Delta T(t)$ is calculated from $P(t_1)$ only, neglecting the second term in (11)

$$\Delta T_0(t)=\frac{1}{C}\int_0^t P(t_1)dt_1\ . \tag{13}$$

Next, $\Delta T_0(t)$, is substituted into the second term of Eq. (11), giving $\Delta T_1(t)$. The operation of substitution of the final result into the second term in Eq. (11) is repeated. The resulting nth order approximation may be written in the form:

$$\Delta T_n(t)=\Delta T_0(t)+\sum_{k=1}^{n-1} S_k(t)\ , \tag{14}$$

where $S_k(t)$ is defined by

$$S_k(t)=(-1)^k\int_0^t\frac{dt_1}{\tau}\int_0^{t_1}\frac{dt_2}{\tau}\cdots\int_0^{t_{k-1}}\frac{dt_k}{\tau}\Delta T_0(t_k)\ . \tag{15}$$

In order to model the $\Delta T(H)$ dependences, the approximation given by Eqs. (14) and (15) should be used. Figures 9 and 10 present results of the numerical calculation. The sum in Eq. (14) is rapidly convergent for $1/\tau\ll 1$, but for $1/\tau=1$, 20 steps of iteration were necessary in order to obtain satisfactory results.

In order to estimate the temperature change, one should note that it depends mainly on the specific heat C_v, the critical current density j_c and the size of the sample D. In $Bi_2Sr_2CaCu_2O_8$ at $T=20$ K, the specific heat is determined mainly by the phonon contribution and is

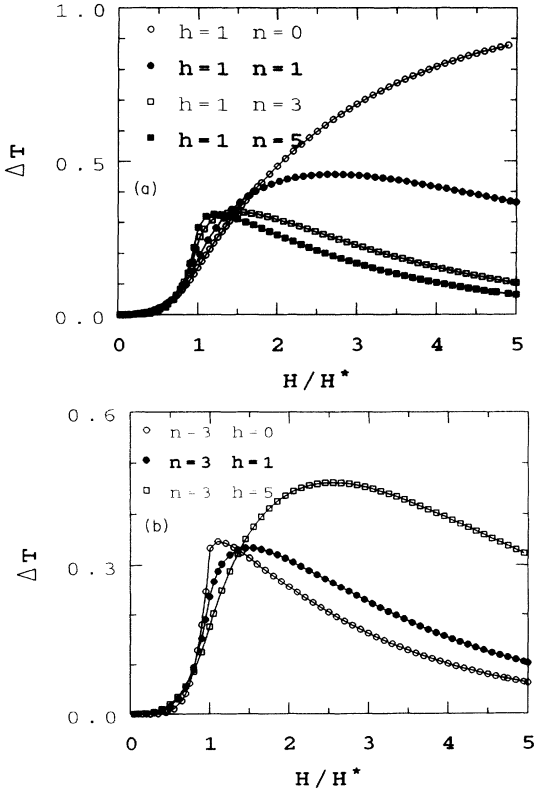

FIG. 9. The temperature change ΔT (in normalized units) as a function of field, when the relaxation time is given by $1/\tau=0.5$. (a) $h=1$ and n changes between 0 and 5, (b) $n=3$ but h changes from 0 to 5.

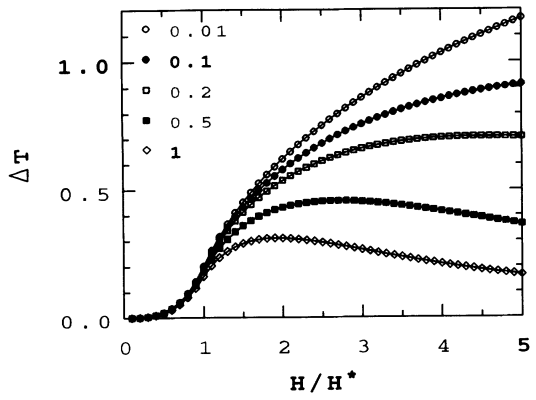

FIG. 10. Temperature change ΔT for different relaxation times, from $1/\tau=0.01$ to 1, when $n=1$ and $h=1$.

about 10 mJ/cm^{3}K. For a sample of the size $5\times6\times2$ mm^3, measurements of $M(H)$ for $H\|c$ give a H^* value of about 15 kOe. From the data in Fig. 15, which correspond to $1/4\tau=0$, $n=1$ and $h=1$, one has in normalized units $\Delta T\approx0.2$ at $H=H^*$, while for $H=5H^*$, $\Delta T\approx1.2$. From these data one calculates temperature changes of about 25 and 150 K. These are upper limits obtained with simplified assumptions, when neither the effect of a temperature or field increase on j_c is considered nor the effect of an increase of temperature on the specific heat. The existence of a thermal link between the sample and its surrounding was also neglected ($\tau\gg1$).

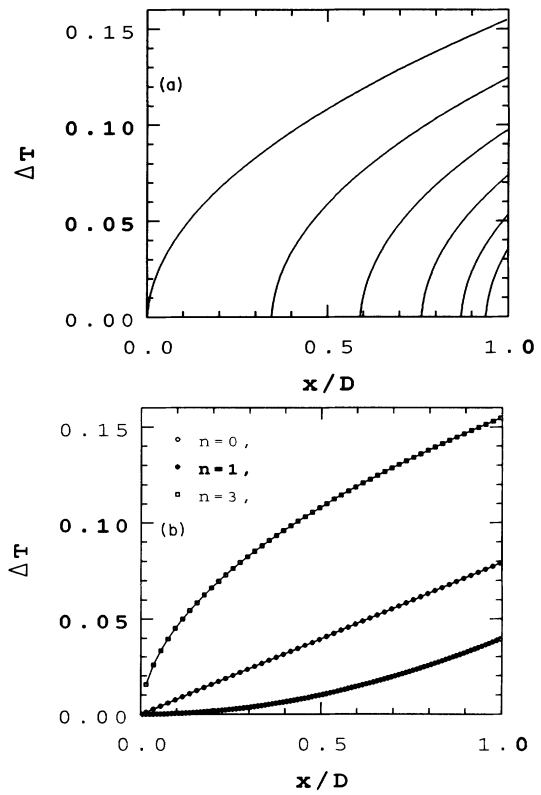

FIG. 11. Temperature distribution in a plate-shaped superconductor exposed to the external field increasing from $H=0$. The calculations are performed for the adiabatic case. (a) Situation at several values of external field, $H/H^*=0.5$, 0.6, 0.7, 0.8, and 1, from right to left, respectively, when $n=1$ and $h=1$. (b) Several curves for different values of n, $n=3$, 1 and 0, from top to bottom, respectively, but $h=1$, when the external field is equal to H^*.

Another possible approximation for the calculation of the sample temperature is based on the assumption of a low, negligibly small thermal conductivity of the sample itself. This approach should be valid when an abrupt field change occurs or in the case of flux jumps, whereas the first method should be used in case of slow variations of the external field. The released power increases the sample temperature locally, with $\Delta T(x,t)=1/C\int P(x,t')dt'$, where $P(x)$ is given by (9) and (10) but with H^* varying, according to the temperature increase. In the following examples, the dependence of H^* on temperature is neglected in the calculations. In Fig. 11 numerical results are presented for several values of the parameters h and n. The strongest temperature increase is found at the sample surface, with the profile $\Delta T(x,t)$ spreading out into the sample center, when the external field increases. For $n=0$, the front profile has a paraboliclike shape, while for large n its curvature is opposite. The largest temperature increase occurs at the sample edge, as discussed by Swartz and Bean.[45] In certain conditions, the flux-jump process starts from the surface, as observed by optical methods.[46,47]

VI. FLUX JUMPS

There is an important connection between the explanation presented in this paper of history-dependent effects in magnetization measurements (irreversibility in $M_{\rm ZFC}(T)$ experiments connected with freezing-in of the flux profile after decrease of temperature) and the phenomenon of flux jumps. If both theories are brought together, the following picture emerges of the flux-profile evolution, which is illustrated schematically in Fig. 12 for the case of quasiadiabatic conditions (i.e., conductivity within the sample and between the sample and the bath are neglected). Curve (a) in Fig. 12 denotes the situation before the occurrence of the jump (j_c is independent of B but a decrease with temperature of j_c is considered). Curve (b) shows a snapshot of a situation within the time interval in which the jump occurs (which happens during a time of the order of 10^{-3} s). The adiabatic profile of $\Delta T(x)$, spreading out from the sample surface, reaches the position x_b, while for $x<x_b$ the temperature is still the same as before. The position x_c is determined from the critical-state ansatz, by the condition that $\int_{x_c}^{D}(dB/dx)dx=H$. Curve (c) presents the situation some time after the jump occurred, when the temperature throughout the sample is uniform and equal to the bath temperature but a non-critical-state flux distribution is frozen-in [as in $M_{\rm ZFC}(T)$ measurements, but after a decrease of temperature]. The current density in the sample volume, corresponding to curve (c) is lower than j_c at the bath temperature, $j\approx j_c(T_{\rm max},H)\ll j_c(T_{\rm bath},H)$. When, after a jump occurred, the external field increases

further—then again a critical-state profile will be built up across the sample (although with a lower j_c than at the beginning of the experiment when H was equal to zero). This will again lead to the initial magnetization change $d(4\pi M)/dH=-1$, as observed in different measurements. Again, a flux jump may occur. The magnetization versus field dependence will resemble a saw shape, as observed in different measurements [e.g., on URu_2Si_2 (Ref. 20) or on $YBa_2Cu_3O_7$ (Ref. 30)]. Hence, knowing the thermal and magnetic parameters of a sample, it is possible to model accurately the evolution of the magnetic-field distribution within the sample during a magnetic instability, as recently carried out by Müller and Andrikidis.[30]

The instability field, H_f, when a flux jump is observed for the first time during virgin magnetization measurements has been given by Swartz and Bean[45] for the case of Bean's critical state and it is related to the temperature dependence of the critical current density and to the volume specific heat. One can write $H_f=H_{j0}$, with H_{j0} given by

$$H_{j0}^2=\frac{8\pi j_0 C_v}{\partial j_0/\partial t}T_c \ . \tag{16}$$

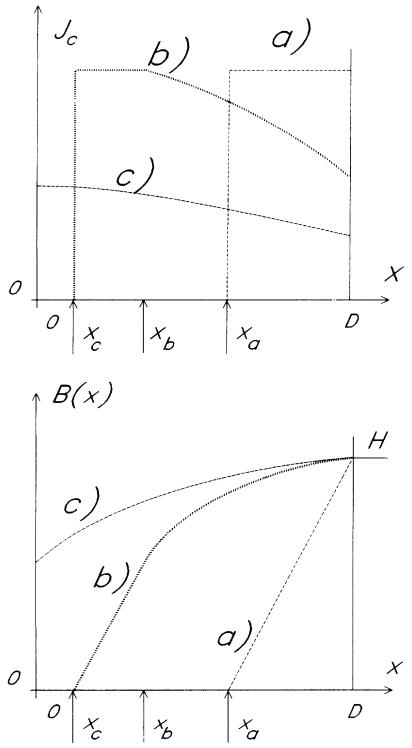

FIG. 12. Possible distribution of current (top figure) and field (bottom figure) when a flux jump occurs. Quasiadiabatic conditions are considered, with a very small sample conductivity. Curves (a) denote a situation before the jump occurred (j_c independent on B is considered, but decreasing with temperature). Curves (b) show a snapshot of a situation within the time interval when the jump occurs. Curves (c) present the situation some time after the jump occurred, when the temperature throughout the sample is uniform and equal to the bath temperature but at which a non-critical-state flux distribution is frozen in.

When the critical current density depends on the magnetic induction, the field H_f is lower than H_{j0}, although the difference is not very large. Recently, Müller and Andrikidis performed calculations for $n=1$ (the classical Kim-Anderson model). We present here the result for the case of arbitrary n, which was derived by following the procedure described in Ref. 30. In order to find H_f, one should solve numerically the equation

$$H_{j0}^2=\frac{2h^2}{2-n}(\mathcal{H}^2-\mathcal{H}^n)+\frac{2h^2}{n-1}(\mathcal{H}-\mathcal{H}^n) \ ,$$
$$\mathcal{H}=1+H_f/h \ , \tag{17}$$

where H_{j0} is given by Eq. (16), in order to find H_f.

In Fig. 13, examples of $H_f(T)$ are given for a few sets of parameters n and m, with the measured specific heat of our sample of URu_2Si_2 [the specific heat has been measured only down to about 400 mK and the linear dependence of C/T on temperature observed up to T_c has been extrapolated down to $T=0$; one should expect a slightly larger value of $C(T)$ at lower temperatures than given by this approximation]. We find that the calculated instability field is lower about 1.5–2 times that the observed one by us (more detailed measurements will be continued) and by Wüchner *et al.*[20] We attribute that to approximations involved in calculation: while modeling of the effects in a large, thin slab is carried out, the measurements have been performed on a cube-shaped sample. Similar problem has been found in earlier attempts to describe quantitatively magnetization and magnetothermal effects simultaneously.[30] We think that a difference for a similar factor between calculations and measurements will be observed on other superconductors also. For instance, the calculations of the temperature dependence of H_f for a few heavy-fermion compounds, shown in Fig. 14, should predict correctly the $H_f(T)$ curves except that the experimental H_f will be about two times larger. The results in Fig. 14 have been calculated with specific heat data as given by Brison *et al.*[48]

The condition for observation of flux jumps is that

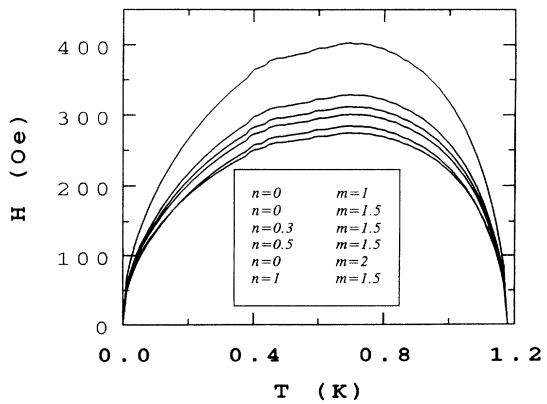

FIG. 13. Calculated temperature dependence of the instability field during virgin magnetization measurements on URu_2Si_2. The parameters n and m, determining the field and temperature dependences of the critical current density are listed in the figure, for curves from top to bottom.

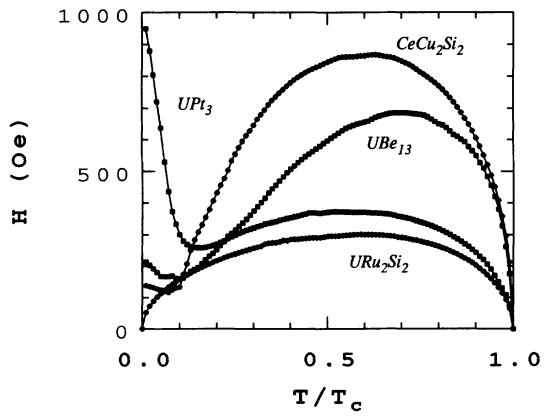

FIG. 14. Calculated temperature dependence of the instability field for a few heavy-fermion superconductors, for parameters $n=0.5$ and $m=1.5$.

$H_f(T)<H^*(T)$. In URu_2Si_2, flux jumps are found below about 500 mK,[20] in agreement with this requirement. In UPt_3, $H^*(T=0)$ is of the order of 10^2 Oe for a millimeter-size sample. Hence, flux jumps will be not observed on this compound [compare with the $H_f(T)$ curve in Fig. 14]. They would be present only for an impractically large sample. For the same reason, one will not be able to find flux jumps in $CeCu_2Si_2$, where the low-field critical current density is only of about 10^3 A/cm^2.[49] We expect that flux jumps will be present in low-temperature measurements on UBe_{13}, where the critical current density is larger than in URu_2Si_2.

The shape of $H_f(T)$ curves at low temperatures is very sensitive to the $C(T)$ and $j_c(T)$ dependence. This observation will be helpful in resolving a few long-standing problems. For instance, it is still unclear if there is an anisotropy in the low-field magnetic properties of URu_sSi_2. Precise measurements of H_{c1} and $j_c(T)$ are very difficult at low fields. However, measurements of $H_f(T)$ at low temperatures for different orientation of field with respect to the crystallographic axes will give a clear indication of the anisotropy of the magnetic properties at low fields. Also, UBe_{13} can be tested in a similar way on the possibility of formation of an anisotropic, unconventional superconducting order parameter.

The calculations of thermal effects under a field-sweep presented above form a basis for a further development of these concepts. Experiments and analytical models of Legrand *et al.*[29] suggest that at short-time scales within which magnetic instabilities occur, a more detailed, noncritical-state description should be used. In many cases, however, the critical-state concept is sufficient for a qualitative analysis of experiments.

VII. SUMMARY AND CONCLUSION

The critical-state theory, with $j_c(B,T)=\alpha(T)/(B+h)^n$, has been used for modeling a number of magnetic properties of superconductors. Calculations of the zero-field-cooled and remanent magnetization are compared with measurements performed on single crystals of $Bi_2Sr_2CaCu_2O_8$ and of the heavy-fermion superconductors UPt_3 and URu_2Si_2. The model allows to explain many experimental results: the occurrence of a peak in the $M(H)$ hysteresis at low fields and saturation of the remanent magnetization as a function of the sample size. Extending the critical-state concept to a description of the flux-profile evolution under changes of temperature allows us to explain history-dependent effects observed during magnetization measurements: the magnetization in certain conditions is found to depend on the external field and temperature only and measurements of $M(H)$ are equivalent to the measurements of $M(T)$. The theory is valuable for computing the magnetocaloric effects in a superconductor exposed to a changing external field and predicts large thermal effects in such experiments.

APPENDIX

In this appendix, the basic results on the magnetization of a superconductor in the modified Kim-Anderson critical-state model will be given. We shall consider the simplest possible geometry: a slab of thickness $2D$, with the external magnetic field H applied along the large surface of this slab (this geometry is chosen to simplify calculations; it is known, however, that the result of this type of calculations depends mainly on some characteristic sample dimension and not so much on the geometry of the sample). As it is explained in the Introduction, the effect of the Meissner state is neglected, which is equivalent to the assumption $H_{c1}=0$. However, more exact calculations[40] do not change significantly the results obtained for $M(H)$, except for certain details.

The aim is to calculate the virgin $M(H)$ curve and the decreasing branch of $M(H)$ after $H_{\max}$ has been applied in the ZFC state. The solution of the differential equation (1), determining the flux distribution, has the form ($x=0$ at the center of the slab):

$$B(x)=\left[\frac{4\pi}{c}\alpha(n+1)|x|+\beta\right]^{1/(n+1)}-h\ , \qquad \text{(A1)}$$

where the integration constant β is determined from the boundary condition $B(\pm D)=H$. For the virgin magnetization curve, β is given by

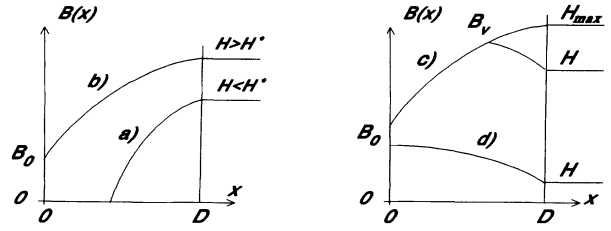

FIG. 15. The magnetic induction distribution in a sample volume when field increases from 0 to $H<H^*$ (a), to $H>H^*$ (b), and when field decreases from $H_{\max}$ to H, in (c) and (d). B_0 is the field at the slab center. B_v is the field at the kink of the flux distribution, occurring for certain range of H values after the sweep direction of H is changed.

$$\beta=(H+h)^{n+1}-(H^*+h)^{n+1}+h^{n+1} . \quad \text{(A2)}$$

Some examples of the flux distribution for different situations are schematically drawn in Fig. 15. In the above equation the following expression for the field H^*, corresponding to the first full penetration of the magnetic field into the center of the slab, is used:

$$H^*=\left[h^{n+1}+\frac{4\pi}{c}\alpha\cdot(n+1)\cdot D\right]^{1/(n+1)}-h . \quad \text{(A3)}$$

An important practical implication of the above result is that H^* weakly depends on the sample size D, for $n>0$ and $h<H^*$.

The magnetization is calculated in a standard way as the spatial average of the magnetic induction over the sample volume, minus the applied field. For the virgin $M(H)$ curve one obtains

$$4\pi M(H)=\frac{n+1}{n+2}\frac{(H+h)^{n+2}-h^{n+2}}{(H^*+h)^{n+1}-h^{n+1}} -h\cdot\frac{(H+h)^{n+1}-h^{n+1}}{(H^*+h)^{n+1}-h^{n+1}}-H ,$$

$$\text{for } H<H^* , \quad \text{(A4)}$$

$$4\pi M(H)=\frac{n+1}{n+2}\frac{(H+h)^{n+2}-(B_0+h)^{n+2}}{(H^*+h)^{n+1}-h^{n+1}} -h\cdot\frac{(H+h)^{n+1}-(B_0+h)^{n+1}}{(H^*+h)^{n+1}-h^{n+1}}-H ,$$

$$\text{for } H>H^* . \quad \text{(A5)}$$

Equation (A4) applies to the situation represented by curve (a) in Fig. 15, while Eq. (A5) applies to the situation represented by curve (b) in this figure.

In Eq. (A5), B_0 is the magnetic induction in the sample center: $B_0=\beta^{1/(n+1)}-h$, with β defined by Eq. (A2). For the decreasing branch of the magnetization, after the maximal field H_{max} has been reached, one obtains

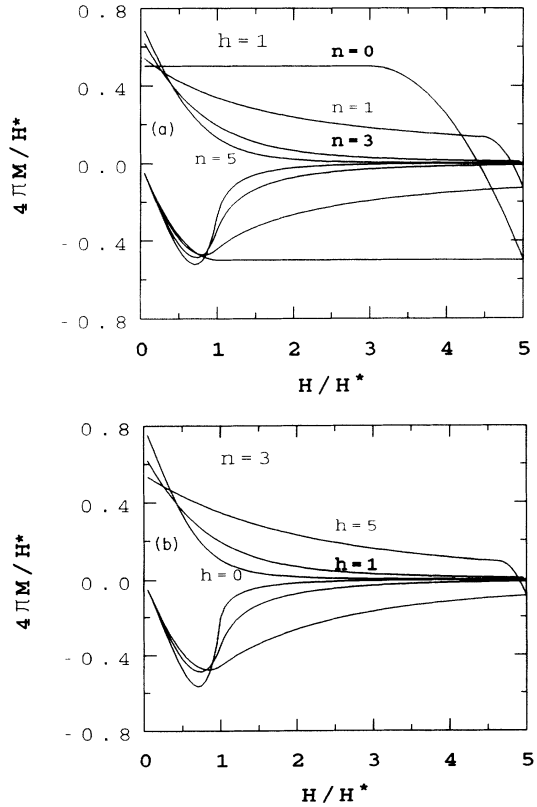

FIG. 16. The calculated virgin magnetization and decreasing branches of the magnetic hysteresis. (a) $h=1$, while n changes from $n=0$ (Bean model) to $n=5$, (b) $n=3$, while h changes 0 to 5. (H and $4\pi M$ are in units of H^*.)

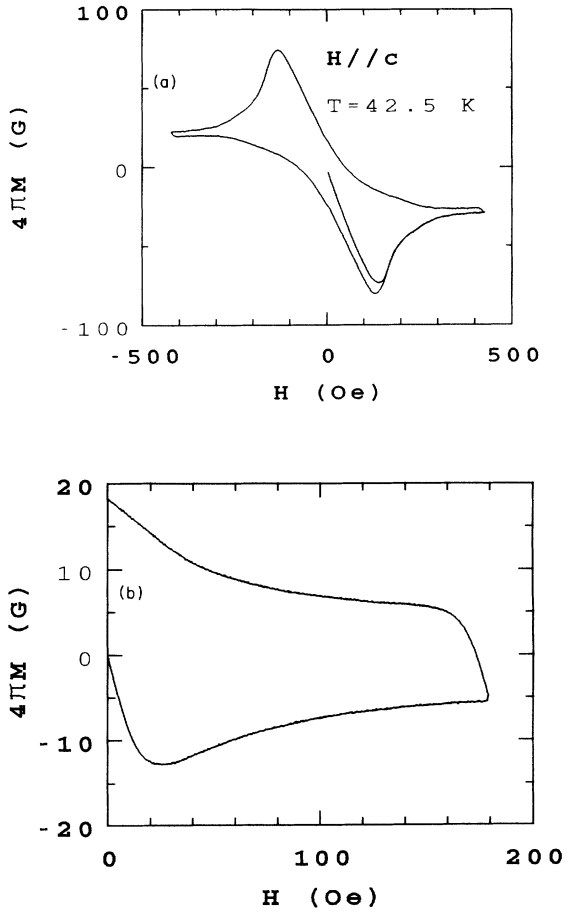

FIG. 17. (a) The magnetic hysteresis of a $Bi_2Sr_2CaCu_2O_8$ single-crystalline sample. The sample has been cooled down from $T>T_c$ in $H=0$ and then the virgin $M(H)$ curve was measured at $T=43$ K and next the whole magnetization hysteresis curve. (b) Magnetization hysteresis (the virgin and decreasing branches) of a UPt_3 sample, measured at $T=448$ mK.

$$4\pi M=\frac{(n+1)/(n+2)[2(B_v+h)^{n+2}-(B_0+h)^{n+2}-(H+h)^{n+2}]-h[2(B_v+h)^{n+1}-(B_0+h)^{n+1}-(H+h)^{n+1}]}{(H^*+h)^{n+1}-h^{n+1}}-H \tag{A6}$$

for $B_v > B_0$ [curve (c) in Fig. 15], and

$$4\pi M=\frac{n+1}{n+2}\cdot\frac{(B_0+h)^{n+2}-(H+h)^{n+2}}{(H^*+h)^{n+1}-h^{n+1}}-h-H \tag{A7}$$

for $B_v < B_0$ [curve (d) in Fig. 15], where B_v is calculated according to

$$B_v=-h+\left[\frac{1}{2}[(H_{\max}+h)^{n+1}+(H+h)^{n+1}]\right]^{1/(n+1)}. \tag{A8}$$

The field B_0 is equal to zero for $H_{\max} < H^*$, and is given by $B_0=\beta^{1/(n+1)}-h$, with β equal to

$$\beta=(H_{\max}+h)^{n+1}-(H^*+h)^{n+1}+h^{n+1} \tag{A9}$$

for $H_{\max} > H^*$ [the case of Eq. (A6)], while β is given by Eq. (A2) in the case of Eq. (A7).

In Fig. 16 some examples of $M(H)$ curves are shown for a few values of the parameters n and h. For the case of a strong field dependence of j_c (when $n>0$ and $h \ll H^*$) the calculated $M(H)$ curves are very similar to those observed for $Bi_2Sr_2CaCu_2O_8$, UPt_3 (Fig. 17) and for other superconductors as, for instance, niobium.[50] The same quite sharp maximum in $M(H)$ is obtained at a field which is comparable, but smaller than H^*, and a nearly reversible behavior in fields that are not much larger than the field that corresponds to this maximum (Fig. 17).

*Electronic address: koziol@phys.uva.nl

[1] C. P. Bean, Phys. Rev. Lett. **8**, 250 (1962).
[2] C. P. Bean, Rev. Mod. Phys. **36**, 31 (1964).
[3] P. W. Anderson, Phys. Rev. Lett. **9**, 309 (1962).
[4] Y. B. Kim, C. F. Hempstead, and A. R. Strnad, Phys. Rev. **129**, 528 (1963).
[5] F. Irie and K. Yamafuji, J. Phys. Soc. Jpn. **23**, 255 (1967).
[6] W. A. Fietz, M. R. Beasley, J. Silcox, and W. W. Webb, Phys. Rev. B **33**, 136 (1964).
[7] H. Ikuta, N. Hirota, Y. Nakayama, K. Kishio, and K. Kitazawa, Phys. Rev. Lett. **70**, 2166 (1993).
[8] M. Xu, D. Shi, and R. F. Fox, Phys. Rev. B **42**, 10 773 (1990).
[9] H. J. Jensen, J. Phys. Condens. Matter **6**, L149 (1994).
[10] S. F. Wahid, N. K. Jaggi, Physica C **194**, 211 (1992).
[11] M. Forsthuber, F. Ludwig, and G. Hilscher, Physica C **177**, 401 (1991).
[12] K.-H. Müller, D. N. Matthews, and N. Driver, Physica C **191**, 339 (1992).
[13] R. Griessen, Wen Hai-hu, A. J. J. van Dalen, B. Dam, J. Rector, H. G. Schnack, S. Libbrecht, E. Osquiguil, and Y. Bruynseraede, Phys. Rev. Lett. **72**, 1910 (1994).
[14] M. Xu, D. Shi, A. Umezawa, K. G. Vandervoort, and G. W. Crabtree, Phys. Rev. B **43**, 13 049 (1991).
[15] L. W. Song, M. Yang, E. Chen, and Y. H. Kao, Phys. Rev. B **45**, 3083 (1992).
[16] H. Yamasaki, K. Endo, S. Kosaka, M. Umeda, S. Yoshida, and K. Kajimura, Phys. Rev. Lett. **70**, 3331 (1993).
[17] D. Dew-Hughes, Philos. Mag. **30**, 293 (1974).
[18] Y. Wolfus, Y. Yeshurun, I. Felner, and H. Sompolinsky, Phys. Rev. B **40**, 2701 (1989).
[19] L. Krusin-Elbaum, A. P. Malozemoff, D. C. Cronemeyer, F. Holtzberg, J. R. Clem, and Z. Hao, J. Appl. Phys. **67**, 4670 (1990).
[20] S. Wüchner, N. Keller, J. L. Tholence, and J. Flouquet, Solid State Commun. **85**, 355 (1993).
[21] Y. B. Kim and M. J. Stephen, in *Superconductivity,* edited by R. D. Parks (Dekker, New York, 1969), Vol. 2.
[22] T. Matsushita, E. S. Otabe, T. Matsuno, M. Murakami, and K. Kitazawa, Physica C **170**, 375 (1990).
[23] J. R. Clem and Z. Hao, Phys. Rev. B **48**, 13 774 (1993).
[24] O. B. Hyun, Physica C **206**, 169 (1993).
[25] M. Xu, Phys. Rev. B **44**, 2713 (1991).
[26] A. Gerber, J. N. Li, Z. Tarnawski, J. J. M. Franse, and A. A. Menovsky, Phys. Rev. B **47**, 6047 (1993); A. Gerber, Z. Tarnawski, V. H. M. Duijn, and J. J. M. Franse, Phys. Rev. B **49**, 3492 (1994).
[27] K. Watanabe, S. Awaji, N. Kobayashi, S. Nimori, G. Kido, K. Kimura, and M. Hashimoto, Cryogenics **32**, 959 (1992).
[28] M. E. McHenry, H. S. Lessure, M. P. Maley, J. Y. Coulter, I. Tanaka, and H. Kojima, Physica C **190**, 403 (1992).
[29] L. Legrand, I. Rosenman, Ch. Simon, and G. Collin, Physica C **208**, 356 (1993); **211**, 239 (1993).
[30] K.-H. Müller and C. Andrikidis, Phys. Rev. B **49**, 1294 (1994).
[31] Z. Koziol, J. J. M. Franse, P. de Chatel, T. Vorenkamp, K. Bakker, and A. A. Menovsky, Physica C **192**, 284 (1991).
[32] Z. Koziol, Ph.D. thesis, University of Amsterdam, 1994.
[33] Lake Shore Cryotronics, Inc., Product Catalog (Cryophysics Limited, Unit 4, Avenue Two, Station Lane Industrial Estate, Witney, Oxford OX8 6YD), 1992.
[34] Z. Koziol and J. J. M. Franse, IEEE Trans. Magn. **MAG-30**, 1172 (1994).
[35] Y. Yeshurun, M. W. McElfresh, A. P. Malozemoff, J. Hagerhorst-Trewhella, J. Mannhart, F. Holtzberg, and G. W. Chandrashekhar, Phys. Rev. B **42**, 6322 (1990).
[36] A. Sulpice, P. Lejay, R. Tournier, and J. Chaussy, Europhys. Lett. **7**, 365 (1988).
[37] K. Kishio, S. Komiya, N. Motohira, K. Kitazawa, and K. Yamafuji, Physica C **185-189**, 2377 (1991).
[38] E. Lähderanta, L. Vlasenko, and R. Laiho, Physica C **190**, 497 (1992).
[39] M. Oussena, P. A. J. de Groot, A. Marshall, and J. S. Abell, Phys. Rev. B **49**, 1484 (1994).
[40] Y. Yeshurun, A. P. Malozemoff, F. Holtzberg, and T. R. Dinger, Phys. Rev. B **38**, 11 828 (1988).

[41]L. Lundgren, P. Nordblad, and L. Sandlund, Europhys. Lett. **1**, 529 (1986).
[42]A. Amato, R. R. Feyerherm, F. N. Gygax, A. Schenck, M. Weber, R. Caspary, P. Hellmann, C. Schank, C. Geibel, F. Steglich, D. E. MacLaughlin, E. A. Knetsch, and R. H. Heffner, Europhys. Lett. **19**, 127 (1992).
[43]W. Braunisch, N. Knauf, G. Bauer, A. Kock, A. Becker, B. Freitag, A. Grütz, V. Kataev, S. Neuhausen, B. Roden, D. Khomskii, D. Wohlleben, J. Bock, and E. Preisler, Phys. Rev. B **48**, 4030 (1993).
[44]M. Sigrist and T. M. Rice, Physica B **186-188**, 866 (1993).
[45]P. S. Swartz and C. P. Bean, J. Appl. Phys. **39**, 4991 (1968).
[46]B. B. Goodman and M. Wertheimer, Phys. Lett. **18**, 236 (1965).
[47]P. Leiderer, J. Boneberg, P. Brull, V. Bujok, and S. Herminghaus, Phys. Rev. Lett. **71**, 2646 (1993).
[48]J. P. Brison, N. Keller, P. Lejay, A. Huxley, L. Schmidt, A. Buzdin, J. Flouquet, D. Jaccard, S. Julian, and G. Lonzarich (to be published).
[49]A. Pollini, A. C. Mota, P. Visani, G. Juri, and T. Terizzi, J. Low Temp. Phys. **90**, 15 (1993).
[50]M. F. Schmidt, N. E. Israeloff, and A. M. Goldman, Phys. Rev. Lett. **70**, 2162 (1993).